

Corrosion Inhibition of Nickel in HCl Solution by Some Indole Derivatives

A.S.Fouda^{1,*}, H.Tawfik², N.M.Abdallah¹ and A.M.Ahmd³

^{1*} Department of Chemistry, Faculty of Science, El-Mansoura University, El-Mansoura- 35516, Egypt,

² Central Chemical Laboratories, Egyptian Electricity Transmission Company, Egyptian Electricity Holding Company, Egypt.

³ Chemistry Department, Faculty of Science, Alex. University, Egypt

E-mail: asfouda@mans.edu.eg

Received: 4 August 2012 / Accepted: 4 February 2013 / Published: 1 March 2013

Some indole derivatives are investigated as corrosion inhibitors for nickel in 0.5 M HCl solution using potentiodynamic polarization and electrochemical impedance spectroscopy (EIS) techniques. A significant decrease in the corrosion rate of nickel was observed in the presence of investigated indole derivatives. Potentiodynamic polarization curves revealed that these inhibitors acted as mixed-type inhibitors, affecting both cathodic and anodic corrosion processes. The adsorption of the inhibitors on nickel surface in 0.5 M HCl was found to follow Frumkin adsorption isotherm. Thermodynamic adsorption parameters (K_{ads} , ΔG°_{ads}) of investigated inhibitors were calculated from the linear form of Frumkin adsorption isotherm. Activation parameters of the corrosion process were calculated and discussed. EIS was used to investigate the mechanism of corrosion inhibition. Correlation between the inhibition efficiency and the structure of these inhibitors are presented.

Keywords: Corrosion inhibition, nickel, HCl, indole derivatives, EIS

1. INTRODUCTION

Nickel is one of the most important metals and it used in a large number of applications. The pure nickel has a good corrosion resistance. Nickel is used as alloying element with other metals. Also, nickel plays an important role in repair or replacement of the diseased bone tissue. The corrosion resistance of nickel is due to the formation of a passive film on its surface upon exposure to the corrosive media. Nevertheless, nickel could be attacked by acidic media in a considerable rate. Acid solutions are commonly used in chemical industry to remove mill scales from metallic surface and because nickel is frequently used in contact with acidic solutions, its corrosion rate must be controlled. One of the useful methods of controlling the corrosion process is the addition of inhibitors. The use of

inhibitors is one of the most practical methods for protection against metallic corrosion, especially in acidic media [1]. The action of inhibition of nickel and its alloys in acidic media by various organic and inorganic inhibitors has been widely studied [2-28]. In general, organic inhibitors such as amines, acetylenic alcohols, heterocyclic compounds, natural rosemary oil, β -aminoketone derivatives, halides, tween surfactants and some phosphonium inhibitors have found use as inhibitors in industrial applications [29- 35].

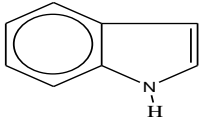
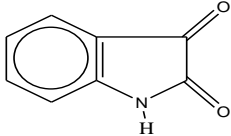
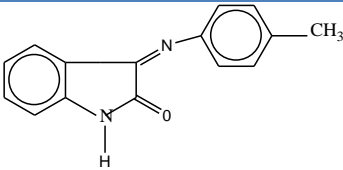
The present work was designed to study the corrosion inhibition of nickel in 0.5 M HCl solution using some indole derivatives as corrosion inhibitors by electrochemical techniques. The synergistic effect brought about by combination of the inhibitors with halides was examined and explained. Also, the effect of temperature on the corrosion behavior was investigated.

2. EXPERIMENTAL METHODS.

2.1 Materials and chemicals

The corrosion tests were performed on nickel rods with a composition (in wt. %): Fe 0.05; Al 0.005; Co 0.005; Mn 0.005, Ti 0.05 and nickel balance. These rods were mounted in Teflon. An epoxy resin was used to fill the space between Teflon and Ni electrode. Rods with an exposed length of 1 cm ($\varphi = 1.25$ mm) were used for all electrochemical measurements. Prior to experiments, all of the electrodes were gradually abraded with different grit emery papers up to 4/0 grit size in order to obtain a smooth surface, degreased with acetone, washing with bidistilled water and finally dried with cool air and stored in a vacuum desiccators.

Table 1. The structures of indole derivatives.

Inhibitor	Inhibitor & Molecular Formula	structure	Molecular Weigh.
(I)	Indole $C_8 H_7 N$		117
(II)	Isatin $C_8 H_5 N O_2$		147
(III)	3-p-tolylimino -1,3-dihydro - indole -2- one $C_{15} H_{12} N_2 O$		237

The aggressive solutions, 0.5 M HCl were prepared by dilution of analytical grade 37 % HCl with bidistilled water. The investigated inhibitors were purchased from SIGMA-ALDRICH and used as received.

Stock solutions (1×10^{-3} M) were made in ethanol to ensure solubility. These stock solutions were used for all experimental purposes. Table 1 shows the molecular structure of investigated inhibitors. It is evident that these investigated inhibitors are heterocyclic inhibitors containing nitrogen and oxygen atoms, which could easily be protonated in acidic solution, and several π -electrons exist in these molecules.

2.2 Methods

Before starting the experiments, the working electrodes were immersed in the test solution for 30 min until a steady potential reached, then the electrochemical measurements were carried out in a conventional three electrodes cylindrical glass cell with a capacity of 100 ml. Saturated calomel (SCE) and a platinum foil were used as reference and auxiliary electrodes, respectively. The reference electrode was connected to a Luggin capillary to minimize IR drop. The polarization curves were obtained potentiodynamically in potential range - 800 mV to + 800 mV versus open circuit potential (E_{OC}) with the scan rate 5 mV s^{-1} .

The inhibition efficiency and surface coverage (θ) were calculated from the following equation:

$$\% \text{ IE} = \theta \times 100 = [1 - (i_{\text{corr(inh)}}/i_{\text{corr(free)}})] \times 100 \quad (1)$$

where ($i_{\text{corr (free)}}$) and ($i_{\text{corr (inh)}}$) are the corrosion current densities in the absence and presence of inhibitors, respectively.

The electrochemical impedance experiments were performed in the frequency range of 100 kHz to 0.5 Hz using a perturbation of 10 mV amplitude at open circuit potential (OCP). The polarization and EIS values of the double layer capacitance (C_{dl}) were calculated from the frequency at which the impedance imaginary component ($-Z_{\text{img}}$) was maximum. Using the following equation:

$$f(-Z_{\text{(img) max.}}) = 1/2\pi C_{dl} R_{ct} \quad (2)$$

% IE was calculated using the following equation:

$$\% \text{ IE} = [(1/R_{ct}) - (1/R'_{ct}) / (1/R'_{ct})] \times 100 \quad (3)$$

where R'_{ct} & R_{ct} are the charge transfer resistance values in the absence and presence of the inhibitors, respectively.

All experiments were conducted at $30 \pm ^\circ\text{C}$. Measurements were performed using Gamry PCI 300/4 Instrument Potentiostat/Galvanostat/ZRA. This includes Gamry Framework system based on the ESA400, Gamry applications that include DC105 for dc corrosion measurements and EIS300 for

electrochemical impedance spectroscopy along with a computer for collecting data. Echem Analyst 5.58 software was used for plotting, graphing and fitting data. All the potentials reported are referred to SCE.

3. RESULTS AND DISCUSSION

3.1 Potentiodynamic polarization measurements

Table 2. Effect of concentration of the investigated inhibitors on the corrosion potential (E_{corr}), corrosion current density (i_{corr}), Tafel slopes (β_a , β_c), degree of surface coverage (θ), inhibition efficiency (% IE) and corrosion rate (C.R.) for the corrosion of nickel in 0.5 M HCl at 30 °C

Comp.	Conc. M	$-E_{\text{corr}}$, mV vs SCE	$i_{\text{corr}} \times 10^4$ A cm $^{-2}$	β_a , mV dec $^{-1}$	β_c , mV dec $^{-1}$	θ	% IE	C.R.
III	0.0	317	4.548	261	254	----	-----	5.32
	3×10^{-6}	210	2.715	207	285	0.403	40.3	3.13
	6×10^{-6}	180	2.249	229	259	0.505	50.5	2.65
	3×10^{-5}	242	2.243	224	284	0.507	50.7	2.60
	6×10^{-5}	236	1.747	204	278	0.616	61.6	2.03
	3×10^{-4}	256	1.262	236	278	0.723	72.3	1.47
	6×10^{-4}	222	0.396	238	260	0.913	91.3	0.46
II	3×10^{-6}	254	2.804	242	284	0.383	38.3	3.26
	6×10^{-6}	212	2.340	256	327	0.485	48.5	2.72
	3×10^{-5}	295	2.312	222	274	0.492	49.2	2.68
	6×10^{-5}	259	1.806	268	285	0.603	60.3	2.10
	3×10^{-4}	206	1.713	247	280	0.623	62.3	1.99
	6×10^{-4}	199	0.627	233	273	0.862	86.2	0.70
I	3×10^{-6}	239	2.998	217	272	0.341	34.1	3.48
	6×10^{-6}	181	2.416	235	260	0.469	46.9	2.81
	3×10^{-5}	217	2.317	232	265	0.491	49.1	2.69
	6×10^{-5}	137	1.865	192	270	0.590	59.0	2.16
	3×10^{-4}	208	1.734	190	283	0.619	61.9	2.01
	6×10^{-4}	318	1.559	291	291	0.657	65.7	1.81

Figure 1 shows typical polarization curves for nickel in 0.5 M HCl solution with and without different concentrations of inhibitor (III) at 30 °C. Similar curves were obtained for other two indole derivatives (not shown). Table 2 collect the associated corrosion electrochemical parameters, i.e. corrosion potential (E_{corr}), corrosion current density (i_{corr}) derived from polarization curves by extrapolation, anodic and cathodic Tafel slopes (β_a & β_c) the degree of surface coverage (θ), as well as the percentage inhibition efficiency (% IE).

It is seen that the addition of investigated indole derivatives shift both the cathodic and anodic branches of the polarization curves of the pure acid solution to lower values of current density

indicating the inhibition of both the hydrogen evolution and nickel dissolution reactions. The corrosion potential is almost unchanged.

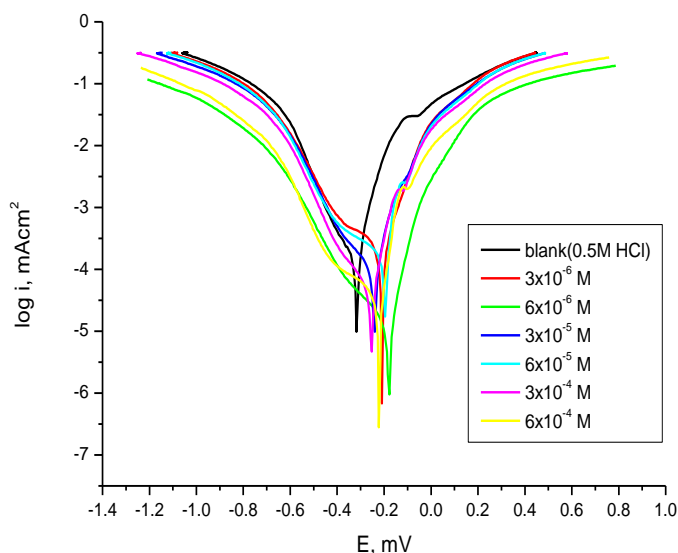


Figure 1. The potentiodynamic polarization curves for the corrosion of nickel 0.5 M HCl in absence and presence of different concentrations of inhibitor (III) at 30°C

These observations indicate that a mixed-type control and investigated indole derivatives are inhibitors of mixed-type for the corrosion of nickel in 0.5 M HCl [36-38]. It is evident that by increasing the inhibitor concentration a decrease in corrosion current densities and an increase in % IE were observed, suggesting that the adsorption protective film tends to be more complete and stable on nickel surface. The anodic and cathodic Tafel slope values are different from the ones obtained with and without the presence of investigated indole derivatives, respectively, suggesting that the mechanism of the reaction of nickel in 0.5 M HCl is influenced by the presence of investigated inhibitors. The higher values of % IE indicate the higher surface coverage, due to the adsorption of inhibitors on the metal surface. The order of decreasing inhibition efficiency of the investigated indole derivatives is as follows: III > II > I.

3.2 Electrochemical impedance spectroscopy (EIS)

The corrosion behavior of nickel in 0.5 M HCl solution in absence and presence of different concentrations of the investigated indole derivatives was investigated by the EIS method at 30°C. Figure (2) shows the Nyquist plots for nickel in 0.5 M HCl solution in the absence and presence of different concentrations of the inhibitor (III) at 30°C. Similar curves were obtained for other two indole derivatives (not shown). These plots having the shape of semicircle for all the concentrations of examined inhibitors indicate that the corrosion is mainly controlled by charge transfer process. The obtained Nyquist impedance diagrams in most cases doesn't show perfect semicircle, generally attributed to the frequency dispersion [39] as a result of roughness and in homogenates of the electrode

surface. The data revealed that, each impedance diagram consists of a large capacitive loop with low frequencies dispersion (inductive arc) which is generally attributed to anodic adsorbed intermediates controlling the anodic process [40-42].

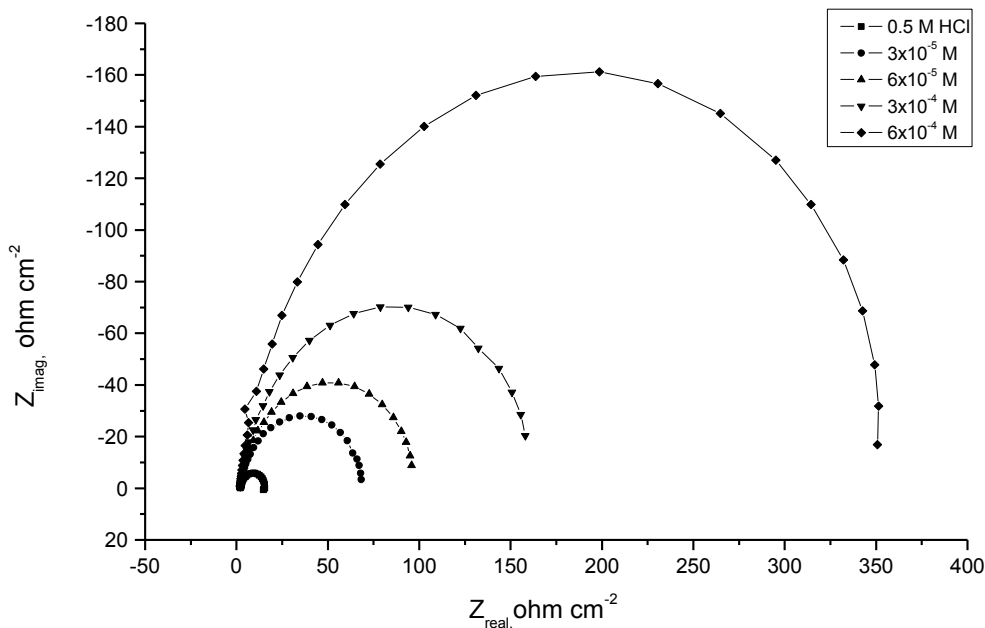


Figure 2. Nyquist plots for nickel in 0.5 M HCl without and with various concentrations of inhibitor (III)

In 0.5 M HCl solution and in the presence of various concentrations of inhibitors, the impedance diagrams show the same trend (one capacitive loop), however, the diameter of this capacitive loop increases with increasing concentration, due to the increase in the number of adsorbed inhibitor molecules when the concentration was raised. From the analysis of Nyquist diagram, the main parameters are the charge transfer resistance R_{ct} , and the capacity of double layer C_{dl} which is defined as:

$$C_{dl} = 1 / (2\pi f_{max} R_{ct}) \tag{4}$$

The surface coverage (θ) and the inhibition efficiencies (% IE) are defined by the following equation:

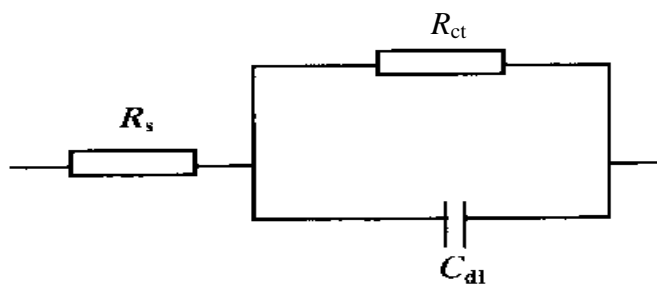
$$\% \text{ IE} = \theta \times 100 = [1 - (R_{ct}^0 / R_{ct})] \times 100 \tag{5}$$

where f_{max} is the maximum frequency, R_{ct}^0 & R_{ct} are the charge transfer resistances in the absence and presence of inhibitor, respectively. The associated parameters with the impedance diagrams are given in Table (3).

Table 3. Electrochemical kinetic parameters obtained by EIS technique for Ni in 0.5 M HCl without and with various concentrations of inhibitors (I- III)

inhibitor	Conc., (M)	C_{dl} $\mu\text{F cm}^{-2}$	R_{ct} Ohm cm^2	θ	% IE
III	0.5 M HCl	16.34	12.62	-	-
	3×10^{-5}	10.04	59.87	0.789	78.9
	6×10^{-5}	8.47	85.51	0.852	85.2
	3×10^{-4}	6.98	144.5	0.913	91.3
	6×10^{-4}	4.79	239.4	0.947	94.7
II	0.5 M HCl	16.34	12.62	-	-
	3×10^{-5}	14.64	22.80	0.446	44.6
	6×10^{-5}	13.27	32.17	0.608	60.8
	3×10^{-4}	10.33	37.71	0.665	66.5
	6×10^{-4}	8.87	43.18	0.708	70.8
I	0.5 M HCl	16.34	12.62	-	-
	3×10^{-5}	17.00	20.21	0.376	37.6
	6×10^{-5}	12.56	24.66	0.488	48.8
	3×10^{-4}	11.11	31.24	0.596	59.6
	6×10^{-4}	10.98	38.57	0.673	67.3

From the impedance results (Table 3) we found that as the inhibitor concentration increased, R_{ct} values increased, but C_{dl} values tended to decrease. The decrease in C_{dl} , which can result from a decrease in local dielectric constant and/or an increase in the thickness of the electrical double layer, suggests that indole derivatives function by adsorption at the metal-solution interface [43]. The change in R_{ct} and C_{dl} values was caused by the gradual replacement of water molecules by the anions of Cl^- and adsorption of the organic molecules on the metal surface, reducing the extent of dissolution [44]. The order of inhibition efficiency obtained from EIS measurements decreases as follows: III > II > I. The % IE obtained from EIS measurements are close to those deduced from polarization measurements. The charge transfer resistance R_{ct} and the double layer capacitance C_{dl} values were derived by using the equivalent circuit, fig. 3.

**Figure 3.** Equivalent circuit model used in the fitting of the impedance data of nickel

3.3 Synergistic effects

The corrosion behavior of Ni in 0.5 M HCl solution in the presence of 10⁻² M KI, KBr and KCl at different concentrations of the investigated inhibitors was studied. From the results of Table (4), it is observed that % IE of the inhibitors increases on the addition of these halides due to synergistic effect of the halide anions and the inhibitors.

Table 4. The effect of concentration of inhibitor (III) on the free corrosion potential (E_{corr}), corrosion current density (i_{corr}), Tafel slopes (β_a& β_c), inhibition efficiency (% IE), degree of surface coverage (θ) and corrosion rate for the corrosion of nickel in 0.5 M HCl + 1x10⁻² M KI, KBr and KCl at 30 °C.

halide	Conc., M	-E _{corr} , mV vs SCE	i _{corr} , x 10 ⁶ A cm ²	β _a , mV dec ⁻¹	β _c , mV dec ⁻¹	θ	% IE	C.R. mmy ⁻¹
KI	0.5 M HCl +1x10 ⁻² M KI	328	0.7660	227	324	0.837	83.7	0.087
	3 x 10 ⁻⁶	119	0.2286	237	212	0.950	95.0	0.003
	6 x 10 ⁻⁶	189	0.1660	185	212	0.964	96.4	0.002
	3x 10 ⁻⁵	142	0.1294	184	198	0.972	97.2	0.002
	6 x 10 ⁻⁵	143	0.1190	192	185	0.974	97.4	0.002
	3 x 10 ⁻⁴	127	0.0504	186	180	0.989	98.9	0.001
	6 x 10 ⁻⁴	107	0.0453	179	175	0.999	99.9	0.001
KBr	0.5 M HCl + 1x10 ⁻² M KBr	263	0.8012	291.5	341.3	0.824	82.4	0.093
	3 x 10 ⁻⁶	170	0.2726	254.8	272.3	0.940	94.0	0.032
	6 x 10 ⁻⁶	178	0.2520	254.2	266.5	0.945	94.5	0.027
	3x 10 ⁻⁵	182	0.1508	233.9	258.0	0.967	96.7	0.018
	6 x 10 ⁻⁵	196	0.1473	227.8	244.1	0.968	96.8	0.017
	3 x 10 ⁻⁴	170	0.0929	240.3	247.0	0.980	98.0	0.012
	6 x 10 ⁻⁴	197	0.0532	243.5	241.2	0.989	98.9	0.011
KCl	0.5 M HCl + 1x10 ⁻² M KCl	202	0.9943	266.8	300.3	0.781	78.1	1.015
	3 x 10 ⁻⁶	277	0.4878	278.3	256.5	0.893	89.3	0.045
	6 x 10 ⁻⁶	266	0.3861	259.8	259.1	0.915	91.5	0.036
	3x 10 ⁻⁵	290	0.2753	257.9	249.4	0.939	93.9	0.032
	6 x 10 ⁻⁵	275	0.2625	255.6	247.4	0.942	94.2	0.031
	3 x 10 ⁻⁴	253	0.1283	250.3	249.1	0.972	97.2	0.023
	6 x 10 ⁻⁴	264	0.744	254.2	251.9	0.925	92.5	0.019

i_{corr} in case of 0.5 M HCl only = 4.548 x 10⁻⁴ A cm⁻²

This may be attributed to the stabilization of adsorbed halide ions by means of electrostatic interactions with the inhibitor, which leads to greater surface coverage (from Cl⁻ to I⁻), thereby, greater

inhibition efficiency. Halide ions are good ligands because they exhibit low electronegativity (< 3.5) [45, 46].

Electronegativity decreases from Cl⁻ to I⁻ (Cl⁻ = 3.0, Br⁻ = 2.8, I⁻ = 2.5), while the atomic radius also increases from Cl⁻ to I⁻ (Cl⁻ = 0.90 °A, Br⁻ = 1.14°A, I⁻ = 1.35°A) [47]. The inhibitor is not adsorbed directly on metal surface itself, but rather by columbic attraction to the adsorbed halide ions on the metal surface. The data in Table (4) indicates that this co-operative effect increased in the order: Cl⁻ < Br⁻ < I⁻, suggesting a possible role by the radii of the halide ions may have an important role to play. The iodide (radius 1.35 °A) ion is more predisposed to adsorption than the bromide ion (radius 1.14°A) and the chloride ion (radius 0.90°A).

3.4 Adsorption isotherms

It is generally assumed that the adsorption of the inhibitors on the metal surface is the essential step in the inhibition mechanism [48].

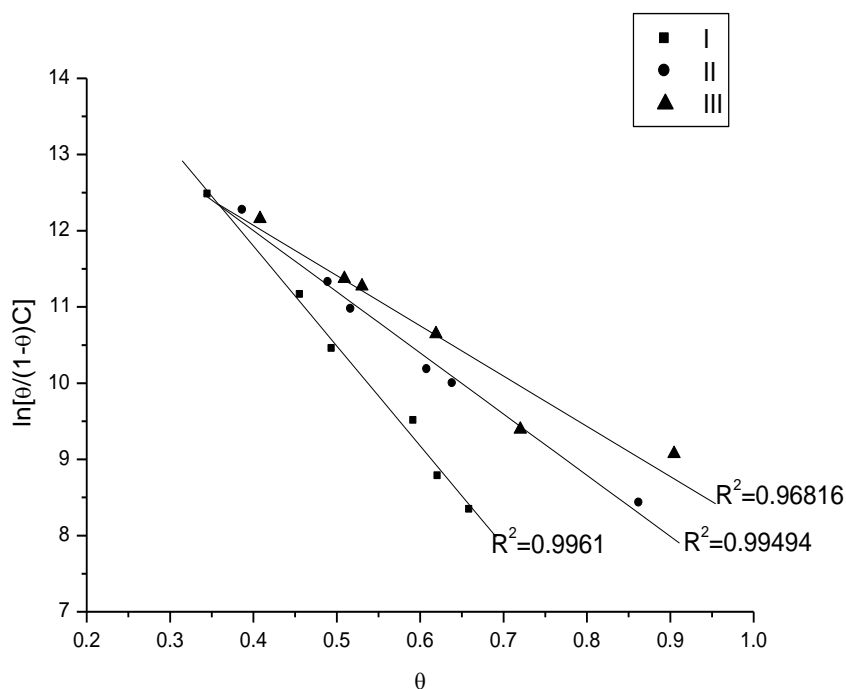


Figure 4. The linear form of Frumkin adsorption isotherm of investigated inhibitors on nickel surface in 0.5 M HCl solution

To determine the adsorption mode, various isotherms were tested and the Frumkin mode should be the best. This Frumkin model has been used for other inhibitor systems [49, 50]. According to this isotherm θ is related to inhibitor concentration via:

$$[\theta / (1-\theta) \exp(-2a\theta) = KC] \tag{6}$$

or its linear form:

$$\ln\left[\frac{\theta}{(1-\theta)C}\right] = \ln K_{\text{ads}} + 2a\theta \quad (7)$$

where a is the interaction parameter between molecules adsorbed on the metal surface and K_{ads} the equilibrium constant of adsorption. Figure 4 represents the linear relationship of the Frumkin adsorption isotherm. By plotting $\ln\left[\frac{\theta}{(1-\theta)C}\right]$ vs. θ , straight lines were obtained for all investigated inhibitors. The equilibrium constant (K_{ads}) is related to the free energy of adsorption ($\Delta G^{\circ}_{\text{ads}}$) by:

$$K_{\text{ads}} = (1/55.5) \exp(-\Delta G^{\circ}_{\text{ads}}/RT) \quad (8)$$

where 55.5 is the molar concentration of water in solution in mol L^{-1} . The slope of the linear fitting of Frumkin gave the values of (a) and the intercepts gave the values of K_{ads} for all the investigated inhibitors (Table 5).

Table 5. Interaction parameters (a), adsorption equilibrium constant (K_{ads}) and free energy ($\Delta G^{\circ}_{\text{ads}}$) of nickel dissolution in 0.5 M HCl in the presence of investigated inhibitors at 30 °C.

Inhibitor	-a	$K_{\text{ads}} \times 10^{-6}$ M^{-1}	$-\Delta G^{\circ}_{\text{ads}}$, kJ mol^{-1}
III	3.3	25.3	52.2
II	4.0	4.0	47.6
I	6.6	2.4	46.4

The negative values of (a) indicates the presence of repulsive forces between the adsorbed species of the investigated inhibitors and the increasing values of K_{ads} from I to III reflects the increasing capability, due to structural formation, on the metal surface [51]. The calculated $\Delta G^{\circ}_{\text{ads}}$ values, using Eq.8, were also given in Table 5. The large negative values of $\Delta G^{\circ}_{\text{ads}}$ ensure the spontaneity of the adsorption process and the stability of the adsorbed layer on Ni surface [52, 53] as well as a strong interaction between inhibitors molecules and the metal surface [54].

Generally, absolute values of $\Delta G^{\circ}_{\text{ads}}$ up to 20 kJ mol^{-1} are consistent with physisorption, while those around 40 kJ mol^{-1} or higher are associated with chemisorptions as a result of the sharing or transfer of electrons from organic molecules to the metal surface to form a coordinate type of metal bond. Here the calculated values of $\Delta G^{\circ}_{\text{ads}}$ are ranging from -52.2 and $-46.4 \text{ kJ mol}^{-1}$, indicating that the adsorption mechanism of the inhibitors on Ni surface in 0.5 M HCl solution at the studied temperatures is due to mixed type of adsorption (electrostatic-adsorption and chemisorptions) [55]. The decrease of % IE with rise in temperature indicates that the physisorption has the major contribution while the chemisorptions have the minor contribution in the inhibition mechanism [56].

Table 6. Effect of 6×10^{-4} M of the investigated indole derivatives on the free corrosion potential (E_{corr}), corrosion current density (i_{corr}), Tafel slopes (β_a & β_c), degree of surface coverage (θ), inhibition efficiency (% IE) and corrosion rate (C.R.) for the corrosion of nickel in 0.5 M HCl at different temperatures.

Temp., °C	Conc. M	$-E_{\text{corr.}}$, mV vs. SCE	$i_{\text{corr.}}$, $\times 10^{-4}$ A cm^2	β_a , mV dec^{-1}	β_c , mV dec^{-1}	θ	% IE	C.R. mmy^{-1}
30	Blank	317	4.55	261	254	----	-----	5.32
	I	318	1.56	291	291	0.657	65.7	1.80
	II	199	2.03	233	273	0.862	86.2	0.70
	III	222	3.96	238	260	0.913	91.3	0.46
40	Blank	271	6.18	286	280	---	---	6.27
	I	247	2.53	256	256	0.591	59.1	3.25
	II	276	2.42	249	256	0.608	60.8	2.84
	III	247	2.37	252	257	0.617	61.7	2.80
50	Blank	206	6.51	297	249	----	----	6.45
	I	251	5.07	304	272	0.221	22.1	6.02
	II	277	4.82	249	283	0.260	26.0	5.72
	III	253	3.71	340	324	0.430	43.0	4.31
60	Blank	287	7.22	310	287	---	---	6.86
	I	307	5.91	305	331	0.181	18.1	6.21
	II	290	5.51	286	274	0.237	23.7	6.17
	III	321	5.17	293	279	0.284	28.4	6.10

3.5 Activation parameters of inhibition process

The influence of solution temperature on the inhibition performance of investigated inhibitors for nickel in 0.5 M HCl solution in the absence and presence of 6×10^{-4} M concentration at temperature ranging from 30 to 60 °C was studied using polarization measurements. The results are presented in Table 6. The results of Table 6 show the increase in solution temperature causes E_{corr} to shift in the positive direction and enhances both the anodic and cathodic reactions. This may be attributed to the fact that an increase in temperature usually accelerates corrosion processes, giving rise to higher metal dissolution rates and a possible shift of the adsorption – desorption equilibrium towards desorption. This as well as roughening of the metal surface as a result of enhanced corrosion, may also reduce the ability of the inhibitor to be adsorbed on the metal surface. The observed decrease in the strength of the adsorption at higher temperatures suggests that physical adsorption may be the main type of adsorption of indole derivatives

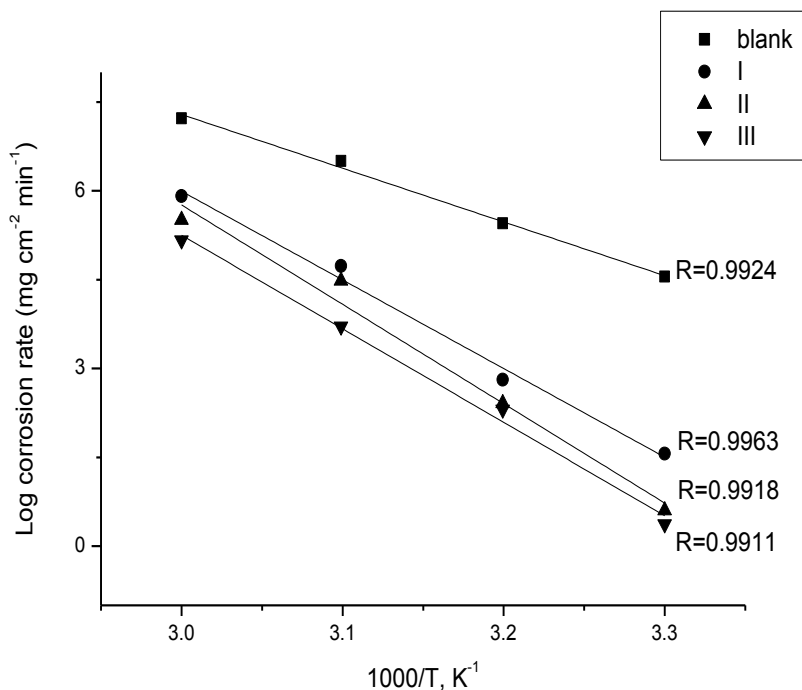


Figure 5. log corrosion rate vs. 1/T curves for the corrosion of nickel in 0.5 M HCl at 6×10^{-4} M for the investigated inhibitors

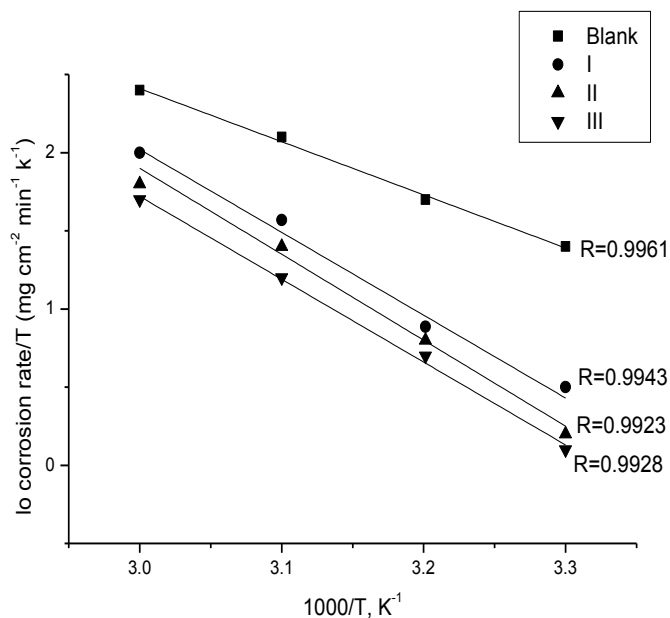


Figure 6. log corrosion rate/T vs. 1/T curves for the corrosion of nickel in 0.5 M HCl at 6×10^{-4} M investigated inhibitors

Plot of logarithm of corrosion rate (log k), with reciprocal of absolute temperature (1/T) for Ni in 0.5 M HCl at 6×10^{-4} M for the investigated indole derivatives is shown in Figure (5). As shown from this Figure, straight lines with slope of $-E_a^*/2.303R$ and intercept of A were obtained according to Arrhenius-type equation:

$$K = A \exp(-E_a^*/RT) \quad (9)$$

where k is the corrosion rate, A is a constant depends on a metal type and electrolyte, E_a^* is the apparent activation energy, R is the universal gas constant and T is the absolute temperature. Plot of $\log(\text{corrosion rate}/T)$ vs. $1/T$ for Ni in 0.5 M HCl at 6×10^{-4} M for the investigated indole derivatives is shown in Figure (6). As shown from this Figure, straight lines with slope of $(-\Delta H^*/2.303R)$ and intercept of $(\log R/Nh + \Delta S^*/2.303R)$ were obtained according to transition state equation:

$$\text{Rate} = RT/Nh \exp(\Delta S^*/R) \exp(-\Delta H^*/RT) \quad (10)$$

where h is Planck's constant, N is Avogadro's number, ΔH^* is the activation enthalpy and ΔS^* is the activation entropy. The calculated values of the apparent activation energy, E_a^* , activation enthalpies, ΔH^* and activation entropies, ΔS^* are given in Table (7). The linear regression coefficients (R^2) are close to unity, indicating that the corrosion of nickel in 0.5 M HCl solution may be elucidated using the kinetic model. These values indicate that the presence of the additives increases the activation energy, E_a^* and the activation enthalpy, ΔH^* and decreases the activation entropy, ΔS^* for the corrosion process. The higher values of, E_a^* , suggest that dissolution of nickel is slow in presence of inhibitors. It is clear that the higher values of E_a^* lead to the lower corrosion rate. Also, the increase in the, E_a^* , indicates strong adsorption of the inhibitor molecules on Ni surface and the presence of energy barrier caused by the adsorption of the additive molecules on Ni surface. The increase in the activation enthalpy (ΔH^*) in the presence of the inhibitors implies that the addition of the inhibitors to the acid solution increases the height of the energy barrier of the corrosion reaction to an extent depends on the type and concentration of the present inhibitor.

Table 7. Thermodynamic activation parameters for the dissolution of Ni in the presence and absence of 6×10^{-4} M of the investigated inhibitors in 0.5 M HCl

Inhibitor	Activation parameters		
	E_a^* , kJ mol ⁻¹	ΔH^* , kJ mol ⁻¹	$-\Delta S^*$, J mol ⁻¹ k ⁻¹
0.5 M HCl	17.4	6.5	177.7
I	30.1	10.2	158.5
II	32.7	10.5	154.7
III	35.9	11.1	145.1

The positive sign of (ΔH^*) indicates the endothermic behavior of these inhibitors at activated states. The entropy of activation (ΔS^*) in the blank and inhibited solutions is large and negative indicating that the activated complex represents association rather than dissociation step [57, 58]. The order of decreasing inhibition efficiency, as observed from the increase in activation energy, is as follows: III > II > I

3.6. Mechanism of corrosion inhibition

Corrosion inhibition of nickel in 0.5 M HCl solution by the investigated indole derivatives as indicated from potentiodynamic polarization and impedance (EIS) techniques was found to depend on the concentration and the nature of the inhibitors.

It is generally, assumed that adsorption of the inhibitor at the metal / solution interface is the first step in the action mechanism of the inhibitors in aggressive acid media. Four types of adsorption may take place during inhibition involving organic molecules at the metal / solution interface [59]:

i) Electrostatic attraction between charged molecules and charged metal ii) Interaction of unshared electrons pairs in the molecule with the metal iii) Interaction of π electrons with the metal and iv) A combination of the above.

Concerning inhibitors, the inhibition efficiency depends on several factors; such as: (a) the number of adsorption sites and their charge density, (b) molecular size, heat of hydrogenation, (c) mode of interaction with the metal surface, and (d) the formation metallic complexes [60].

Most organic inhibitors contain at least one polar group with an atom of nitrogen, sulfur or oxygen, each of them in principle representing an adsorption center. The inhibitive properties of such inhibitors depend on the electron densities surrounding the adsorption centers: the higher the electron density at the center, the more the effective the inhibitor. Also, it is apparent that the adsorption of these inhibitor molecules on the nickel surface could occur directly on the basis of donor-acceptor behavior between the lone pairs of the heteroatom and the extensively delocalized π -electrons of the inhibitor molecule and the vacant d-orbital of iron surface atoms [61]. These inhibitors are able to adsorb on anodic sites through N, O atoms, heterocyclic and aromatic rings which are electron donating groups. The adsorption of these inhibitors on anodic sites may decrease anodic dissolution of nickel. In the aqueous acidic solutions, most of organic inhibitors containing N atoms exist either as neutral molecules or in the form of cations (protonated). In general two modes of adsorption could be considered. In our case, the neutral form is the preferable one, the inhibitor molecules may adsorb on the Ni surface via the chemisorption mechanism, involving the displacement of water molecules from the metal surface and the sharing electrons between the N, and O atoms and Ni. The order of increased inhibition efficiency for indole derivatives is: III > II > I as indicated from the different methods.

Inhibitor (III) is the most efficient inhibitor. This is due to its larger molecular size, the presence of two N atoms, O atom and CH₃ in the p-position which has higher electron donation character. On the other hand, inhibitor (I) is the least effective inhibitor in this series. This is due to the presence of one N atom and it has the lowest molecular size. Inhibitor (II) comes after inhibitor (III) in the inhibition efficiency. This is due to the presence of one N atom, two O atoms and lower molecular size than inhibitor (III).

4. CONCLUSIONS

In this paper, electrochemical methods were used to study the ability of indole derivatives to inhibit the corrosion of nickel in 0.5 M HCl solution. The principal conclusions are:

1) The inhibition efficiency of indole derivatives increases by increasing the inhibitor concentration, but it decreases with increase in temperature.

2) The polarization curves indicated that indole derivatives inhibit both cathodic hydrogen evolution and anodic metal dissolution reactions. These derivatives act as mixed-type inhibitors.

3) Ac impedance plots of nickel indicated that polarization resistance increases with increase in inhibitor concentration.

4) The adsorption of these inhibitors on the metal surface from 0.5 M HCl solution obeys Frumkin adsorption isotherm. The negative sign of $\Delta G^{\circ}_{\text{ads}}$ indicates that the adsorption process is spontaneous.

5) The increase in activation energy after the addition of inhibitors to the 0.5 M HCl solution indicates that the adsorption is more physical than chemical.

6) On addition of halide anions to 0.5 M HCl containing inhibitors, a synergistic or cooperative effect occurred thus inhibiting nickel corrosion.

References

1. H.G.Feller, H.G.Ratzer Scheibe, *Electrochim.Acta*, 17(1972)17
2. H.G.Feller, H.G.Ratzer Scheibe, W.Wendt, *Electrochim.Acta*, 18(1973)175
3. H.G.Feller, M.Kesten, J.Krupski, *Proc.Int.Congr.Corros.*, 515(1974)155
4. H.G.Feller, M.Kesten, H.G.Ratzer Scheibe, *Proc.5th Int.Comgr.Metal Corrosion*, 149(1974)
5. M.C.Petit, A.Jouanneau, *Proc. 5th Int.Comgr.Metal Corrosion*, 237(1974)
6. I.Graz, B.Galzer, *Corros.Sci.*, 14(1974)253
7. L.A.Barkalatsova, A.G.Pshenicknikov, *Electrochem.*, 12(1976)42
8. N.A.Balashova, N.T.Gorokova, M.I.Kulesnova, S.A.Libin, *D.C.Soobsch*, 3(1976)264
9. M.Kesten, *Corrosion*, 32(1976)94
10. I.L.Soruskhim, G.A.Tedoradze, G.I.Kaurova, T.I.Raxmerova, *Electrokhim.*, 12(1976)442
11. E.I.Mikhailova, Z.A.Iofa, *Ind.J.Chem.*, 12(1974)664
12. H.Breushke, F.Weller, K.H.Ebert, *Werk.U.Korros.*, 27(1974)664
13. A.M.Maitra, K.Bhattacharyya, *J.Ind.Chem.Soc.*, LVI(1979)1202
14. A.S. Fouda, A. Al-Sarawy and T. M. Omar, *Annali di chim.*, 95 (2005) 53.
15. A.S. Fouda, A. A. El-Shafei and H. E. Gadow, *Port. Electrochim.Acta*, 20 (2002) 13
16. A.S. Fouda, H. E. Gadow and A. A. El-Shafei, *KorroziosFigyelo*, 43 (3) (2003) 95
17. G. Schmit, *Br. Corros. J.*, 19(4) (1984) 465
18. G. Lewis, *Corros. Sci.*, 22 (1982) 579
19. S. Rengamani, I. Vasudvan and S. V. K. Lyer, *IND. J. Technol.*, 31 (1993) 519.
20. M. Stern and A. I. J. Geary, *J. Electrochem. Soc.*, 104 (1957) 56
21. A.K. Maayta and N. A. F. Rawshdeh, *Corros.Sci.*, 46 (2004) 1129
22. A.A. Aksut, S. Bilgic, *Corros. Sci.*, 33 (1992) 379.
23. E. Khamis, F. Bellucci, R.M. Latanision, E.S.H. El-Ashry, *Corrosion*, 47 (1991) 677.
24. S.M. Reshetnikov, *Port. Met.*, 14 (1978) 491.
25. V. Sastry, R. Packwood, *Werkst. Korros.*, 38 (1987) 77.
26. A.Frignani, C. Monticelli, G. Trabaneli, *Br. Corros. J.*, 33 (1998) 71.
27. C.F. Zinola, A.H. Castro Luna, *Corros. Sci.*, 37 (1995) 1919.
28. K. Bajpai, G. Singh, *Bull. Electrochem.*, 16 (2000) 241.
29. A.S. Fouda, G. Y. Elewady and K. Shalabi, *Mansoura J. Chem.*, 35(2) (2008) 35.
30. T.Tsuru, S. Haruyama and G. Boshku, *J. Jpn. Soc. Corros. Eng.* 27 (1978) 573

31. M.Abdallah, S.O.Alkaranee, A.A.Abdel Fattah, *ZSastita Materijala*, 50(2009)205-212
32. G.Y.Elewady, A.El-Askalany, A.F.Molok, *Port.Electrochim.Acta*, 26(6)(2008)503-516
33. M.Abdallah, A.Y.El-Etre, *Port.Electrochim.Acta*, 21(2003)315-326
34. S.Hinnov, J.Tamm, *Chemistry*, 60(3)(2011)184-192
35. M.Walia, G.Singh, *Surf.Eng.*, 21(3)(2005)176-179
36. E.S.Ferreira, C.Giancomlli, F.C.Giancomlli and A.Spinelli, *Mater.Chem.Phys.*, 83 (2004) 129
37. L.J.Vracar and D.M.Drazic, *Corros.Sci.*, 44 (2002) 1669
38. X.H.Liand S.D.Deng, *Corros.Sci.*, 509 (2008) 420.
39. T. Paskossy, *J. Electroanal. Chem.*, 364 (1994) 111
40. J. Bessone, C. Mayer, K. Tuttner and W. Lorenz, *J. Electrochim. Acta.*, 28 (1983) 171
41. A.Caprani, I. Epelboin, Ph. Morel and H. Takenouti, Proceedings of th 4th European Sym. On Corrosion Inhibitors, Ferrara, Italy, 571(1975).
42. I.Epelboin, M. Keddam and H. Takenouti, *J. Appl. Electrochem.*, 2 7 (1972) 1
43. E.McMcCafferty, N.Hackerman, *J.Electrochem.Soc.*, 119(1972) 146.
44. S.Muralidharan, K.L.N.Phani, S.Pitchumani, S.Ravichandran, *J.Electrochem.Soc.*, 42 (1995) 1478
45. K.Snyder, *Chem.Struct.React.*, 2(1966)120
46. G.K.Gomma, *Mater.Chem.Phys.*, 55 (1998) 243.
47. R.M.Tennent (Ed), Science Data Book, *Oliver & Boyd, Edinburgh*, 1978, p.56
48. A.Asan, M.Kabasakaloglu, M.Isiklan and Z.Kilic, *Corros.Sci.*, 47 (2005) 1534.
49. A.S.Fouda, M.Abdallah and R.A.El-Dahab, *Desalination and Water Treatment*, 22(2) (2010) 340
50. A.S.Fouda,S.T.Shawagfeh, *Bull.Soc.Chim.Fr.*, 127 (1990) 30.
51. S.I.Da Costa, and S.M.L.Agostinho, *J.Electroanal.Chem.*, 196(1) (1990) 51.
52. L.Tang, X.Li, L.Lin, G.Mu, and G.Liu, *Mater.Chem.Phys.*, 97 (2006) 301.
53. K.Tebbji, N.Faska, A.Tounsi, H.Ouddad ,M.Benkaddour and B.Hammouti, *Mater.Chem.Phys.*, 106 (2007) 2144.
54. G.Mu, X.Li, and G.Liu, *Corros.Sci.*, 47 (2005) 1932.
55. S.A.Ali, H.A.Al-Muallem, M.T.Saeed and S.U.Rahman, *Corros.Sci.*, 50 (2008) 664.
56. E.A.Noor, and A.H.Al-Moubaraki, *Corros.Sci.*, 51 (2009) 868.
57. G.K.Gomma and M.H.Wahdan, *Mater. Chem. Phys.*, 30 (1995) 209
58. M.S. Soliman and Ph. D. Thesis, *Alex. Univ., Egypt* (1995).
59. D.Schweinsberg, G.George, A.Nanayakkara and D.Steiner, *Corros.Sci.*, 28 (1988) 55.
60. A.S.Fouda, M.N.Mousa, F.I.Taha and A.I.Elneanaa, *Corros.Sci.*, 26(1986)719.
61. S.Muralidharan, M.A.Quraishi, and SV.K.Iyer, *Corros.Sci.*, 37(1995)1739.